Novel process to prepare magnetic metal-ceramic nanocomposites from zeolite precursor and their use as adsorbent of agrochemicals from water

Title: Novel process to prepare magnetic metal-ceramic nanocomposites from zeolite precursor and their use as adsorbent of agrochemicals from water

Authors: Michele Pansini, Filomena Sannino, Antonello Marocco, Paolo Allia, Paola Tiberto, Gabriele Barrera, Michelangelo Polisi, Edmondo Battista, Paolo Antonio Netti, Serena Esposito

PII: S2213-3437(17)30669-3
DOI: https://doi.org/10.1016/j.jece.2017.12.030
Reference: JECE 2077

To appear in:

Received date: 14-10-2017
Revised date: 4-12-2017
Accepted date: 15-12-2017

Please cite this article as: Michele Pansini, Filomena Sannino, Antonello Marocco, Paolo Allia, Paola Tiberto, Gabriele Barrera, Michelangelo Polisi, Edmondo Battista, Paolo Antonio Netti, Serena Esposito, Novel process to prepare magnetic metal-ceramic nanocomposites from zeolite precursor and their use as adsorbent of agrochemicals from water, Journal of Environmental Chemical Engineering https://doi.org/10.1016/j.jece.2017.12.030

Novel process to prepare magnetic metal-ceramic nanocomposites from zeolite precursor and their use as adsorbent of agrochemicals from water

Michele Pansini[1], Filomena Sannino[2], Antonello Marocco[1], Paolo Allia[3], Paola Tiberto[4],Gabriele Barrera[4], Michelangelo Polisi[5],Edmondo Battista[6,7], Paolo Antonio Netti[6,7], Serena Esposito[1]*

[1]Department of Civil and Mechanical Engineering and INSTM Research Unit, Università degli Studi di Cassino e del Lazio Meridionale, Via G. Di Biasio 43, 03043 Cassino, FR, Italy.

[2]Department of Agricultural Sciences, University of Naples "Federico II", Via Università 100, 80055 Portici, NA, Italy.

[3]Department of Applied Science and Technology and INSTM Unit of Torino-Politecnico, Politecnico di Torino, Corso Duca degli Abruzzi 24, 10129 Torino, Italy.

[4]INRIM, Nanoscience and Materials Division, Strada delle Cacce 91, 10135 Torino, Italy.

[5]Dipartimento di Scienze Chimiche e Geologiche, Università degli Studi di Modena e Reggio Emilia,Via Campi 103, 41125 Modena, Italy.

[6]Interdisciplinary Research Centre on Biomaterials (CRIB) and Dipartimento di Ingegneria Chimica, dei Materiali e della Produzione Industriale (DICMAPI), University of Naples Federico II, Piazzale Tecchio 80, 80125, Napoli, Italy.

[7]Center for Advanced Biomaterials for Health Care@CRIB Istituto Italiano di Tecnologia, Largo Barsanti e Matteucci 53, 80125 Napoli, Italy

Corresponding author: Serena Esposito email: s.esposi@unicas.it, Tel: +39 07762993697, Fax: +39 07762993711

Graphical Abstract

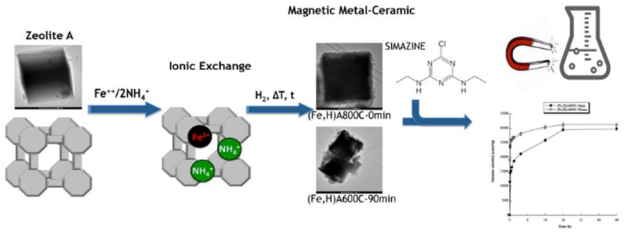

Abstract

In this work the preparation of two samples of magnetic adsorbent from a zeolite precursor was described. This process implied NH_4^+ and Fe^{2+} exchange of zeolite A and its subsequent thermal treatment at temperature 600-800 °C, under a reducing atmosphere. These two magnetic adsorbents, composed of Fe/Fe_3O_4 nanoparticles embedded in an amorphous silica-alumina ceramic phase,were fully characterized by determining their chemical composition, quantitative phase analysis, surface area, SEM and TEM analysis, pH of zero potential and magnetic properties. In particular, their Fe content was 0.2 or 4.8%, Fe_3O_4content 5.4 or 7.1 % and the average dimension of nanoparticles was 1.82 or 11.13 nm. Then, the removal of the agrochemical simazine from water was performed by using these two magnetic adsorbents. The investigated parameters were pH, time, solid/liquid ratio and initial simazine concentration. The pH of maximum simazine adsorption was 6.5 and 3.0 for the two adsorbents. At these pH values, simazine adsorption occurred rapidly and massively even from very dilute simazine solutions (simazine concentration of about 0.25 µmole/L).

Finally, a process of simazine removal from waters based on repeated cycles of adsorbent addition to simazine bearing water, followed by its easy magnetic separation, is proposed. This process allows bringing the final agrochemical concentration well below 0.05 mg/L, the maximum agrochemical concentration allowed by Italian laws in wastewaters. Simazine bearing exhausted

adsorbents are regenerated by a (no more than) 5 min thermal treatment at 300 °C, which results in the decomposition of simazine without damage of the adsorbent.

Keywords: Magnetic adsorbent, metal-ceramic nanocomposites, agrochemical removal, zeolite precursor, iron/magnetite nanoparticles

1. Introduction

Most of the adverse events that can damage the quality of the various crops are usually tackled through the use of agrochemicals. Nevertheless, these chemicals are known to be very harmful for the health of human beings as they may give rise to serious health effects to nervous system, eyes, brain and bone marrow. Moreover, agrochemicals may promote carcinogenic, mutagenic and teratogenic effects [1].

Various methods were proposed for the removal of agrochemicals, including adsorption, sedimentation, membrane filtration, oxidation, photochemical or photocatalytic degradation, biochemical decomposition, and coagulation [1-18]. Many papers suggest adsorption as a method for removal owing to its efficiency, intrinsic simplicity and low costs [1-8].

These considerations, together with a sound experience in the environmental uses of zeolites [19-24], promoted a long term study on simazine removal from water by adsorption on zeolite H-Y and porous silica, which were directly added to the water containing simazine [25-30]. Among the various agrochemicals, simazine (2-chloro-4,6-bis(ethylamino)-*s*-triazine, molecule length = 1.034 nm, molecule width = 0.749 nm [15], Scheme 1) was chosen to represent this class of chemical compounds as it is a synthetic s-triazine herbicide used for pre-emergence control of broad-leaf weeds and annual grasses in agricultural and non-crop fields [12-13] and is known to be the second most

commonly detected pesticide in surface and groundwater in the USA, Australia and Europe [14] and to cause increasing concern [15].

Our recent studies may represent, in a sense, a point of discontinuity with the current literature, which reports data regarding agrochemicals removal from waters by using specific adsorbents. These data are subsequently elaborated in terms of equilibrium and kinetic modelling, sometimes allowing new insight to be gained into the complex interactions occurring between the agrochemical molecules and active sites. Our recent studies went beyond fulfilling these goals, in order to take into account some aspects which are usually neglected, in the following ways:

1) The residual agrochemical concentration in the water was compared with a law limit such as the maximum agrochemicals limit allowed by Italian laws in wastewaters to be released in surface waters or in sink (0.05 mg/L, DLGS. N. 152/2006, from this point onward law limit).
2) The regeneration of the exhausted adsorbent was studied.
3) The final fate of the agrochemical removed from the water was studied.

The results obtained were decidedly encouraging. The residual agrochemical concentration in the water was brought below the law limit through an iterative process which implied several adsorption steps at a very low adsorbent/water ratio (solid/liquid, S/L = 1/10,000 g/g) and some adsorption step at a higher S/L. Then, the problems of the regeneration of the exhausted adsorbent and the final fate of the agrochemical removed from the water were simply solved by a few minutes' thermal treatment of the exhausted adsorbent at about 300 °C, which resulted in the thermal decomposition of simazine. However, a point of weakness of the procedures proposed in this study may be found in the difficulties arising from the separation of the exhausted adsorbent from water. We did this operation by centrifugation, which cannot be proposed at an industrial level. This consideration suggested us to test some magnetic metal-ceramic nano-composite as adsorbent of simazine from water. Such magnetic metal-ceramic nano-composite materials, which could be easily separated from the water containing simazine by the action of an external magnet, were produced starting from a zeolite

precursor following a patented process [31-34]. According to it, Fe^{2+} or Ni^{2+}exchanged commercial zeolites (precursors) were thermally treated at relatively moderate temperatures (500-850 °C), under a reducing atmosphere. During such thermal treatments, the original zeolite structure is almost totally destroyed, thus the product of these operations is a composite formed by a dispersion of metallic Fe or Ninanoparticles in a mainly amorphous silica and alumina matrix.Such magnetic metal-ceramic nano-composite materials were already successfully used in the separation of the *Escherichia coli* DNA from crude cell lysate [35].

On the basis of these considerations, the patented procedure of production of magnetic metal-ceramic nanocomposite materials was slightly modified by inserting an NH_4^+ ion exchange step, in order to make the final products of the process more proper for agrochemical removal. Actually the subsequent thermal treatment of the $Fe^{2+}$and NH_4^+ exchanged zeolite A under reducing atmosphere gives rise to Fe^{2+} reduction to metallic Fe and ammonia evolution with the formation of acid hydrogen sites, which should exhibit a good affinity toward the lone electron pair of nitrogen atoms of the lateral chain present in the basic simazine molecule.

The choice of zeolite A was dictated by:

1) Its high cation exchange capacity due to its Si/Al = 1.00 [36-37].
2) Its low cost, as a result of its widespread use in many technological sectors [36-37].

Finally, this work reports the preparation of two different samples of magnetic adsorbents, their characterization, and data concerning simazine removal from water. Regarding this last topic, points investigated are: i) evaluation of the ability of the samples of magnetic adsorbents in the removal of simazine from water as related to the law limit by investigating the main process parameters (pH, time, initial simazine concentration); ii) proposal of a proper regeneration procedure of the exhausted adsorbent, ensuring depletion of the agrochemical; iii) definition of an iterative process of simazine removal from waters and regeneration of the exhausted adsorbent.

2. Experimental

2.1 Materials

Carlo Erba reagent grade synthetic zeolite 4A (framework type LTA, $Na_{12}Al_{12}Si_{12}O_{48}\cdot 27H_2O$) was used in this study. Exchange solutions were prepared dissolving Carlo Erba reagent grade 99.5 wt.% $FeSO_4\cdot 7H_2O$ andNH_4Cl in doubly distilled water.Reagent grade 2-chloro-4,6-bis(ethylamino)-1,3,5-triazine (simazine, Scheme 1)(99.0% purity) was from Sigma-Aldrich Chemical Company.

2.2 Preparation of the Metal-Ceramic Nanocomposites

In Fig. 1 the procedure followed in preparing the metal-ceramic nanocomposites is outlined. A first sample of metal-ceramic nanocomposite was produced as follows. Zeolite A was contacted with a $[NH_4^+]$ = 0.1 M solution at a wt. solid/liquid ratio of (S/L) = 1/50 g/g, room temperature and contact time (t) = 1 h. The solid was separated from the liquid through filtration and contacted again with a fresh solution. This operation was iterated two times. Then this sample of NH_4^+ exchanged zeolite A was contacted with a $[Fe^{2+}]$ = $[NH_4^+]$ = 0.1 M solution at a wt. solid/liquid ratio of (S/L) = 1/50 and contact time (t) = 1 h. In this exchange the temperature (T) was ≈ 7 °C and Ar was bubbled through the solution to prevent Fe^{2+} oxidation [38] .The solid was separated from the liquid through filtration and contacted again with a fresh solution. This operation was iterated two times. The resulting powders were washed with doubly distilled water, dried for about one day at 80 °C, and stored for at least 3 days in an environment with about 50% relative humidity to allow water saturation of the zeolite. This sample of NH_4^+ and Fe^{2+} exchanged zeolite A was subjected to the following thermal treatment under a reducing atmosphere (created by a flow of a H_2-Ar gaseous mixture, containing 2 vol. % H_2) in an Al_2O_3 tubular furnace (inner diameter = 6.9 cm, height = 91 cm), using Pt crucibles: heating from room temperature up to 800 °C (15 °C/min heating rate); as soon as the temperature of 800 °C was reached, the heating system of the furnace was switched off and the sample was left to cool down to room temperature within the furnace. This sample will be hereafter referred to as (Fe,H)A800C-0min.

A second sample of metal-ceramic nanocomposite was produced as follows. Zeolite A was contacted with a [NH_4^+] = 0.1 M solution according to the same procedures of the previous sample. This exchange was iterated ten times. Then this sample of NH_4^+ exchanged zeolite A was contacted with a [Fe^{2+}] = 0.1 M solution at a wt. solid/liquid ratio of (S/L) = 1/50 g/g, temperature (T) ≈ 7 °C, contact time (t) = 1 h and under Ar bubbling. This operation was iterated eight times. The resulting powders were washed, dried and kept as in the previous case. This sample of NH_4^+ and Fe^{2+} exchanged zeolite A was subjected to the following thermal treatment under a reducing atmosphere: heating from room temperature up to 600 °C (15 °C/min heating rate) and subsequent thermal treatment at 600 °C for 90 min; then the heating system of the furnace was switched off and the sample was left to cool down to room temperature within the furnace. This sample will be hereafter referred to as (Fe,H)A600C-90min.

2.3 Characterization of the Metal-Ceramic Nanocomposites

The Fe^{2+}, $NH_4^+$and residual Na^+ content of Fe and NH_4^+ exchanged zeolite A samples were determined by AAS (Perkin-Elmer Analyst 100) after chemical dissolution of samples [39-40]. The NH_4^+content of Fe and NH_4^+exchanged zeolite A samples was calculated as the difference between the value of the cation exchange capacity of zeolite A (5.48 meq/g) and the sum of Fe^{2+} and residual Na^+ content previously determined.

Zeolite Na-A, samples of Fe and NH_4^+exchanged zeolite A, and samples of the metal-ceramic nanocomposites (Fe,H)A800C-0min and (Fe,H)A600C-90min were characterized by X ray powder diffraction (XRPD, Philips X'Pert diffractometer, Cu Kα radiation). Data were collected by varying the 2θ between 5 and 100° with 0.02° steps. For each step the data was collected for 1 s [41-42].

Quantitative phase analyses were performed on the metal-ceramic nanocomposites (Fe,H)A800C-0min and (Fe,H)A600C-90min, by using synchrotron radiation powder diffraction. The synchrotron XRPD experiments were performed on the high-resolution beamline ID22 at ESRF (Grenoble), with a fixed wavelength of 0.41067 Å. The powders were packed along with Al_2O_3 (10 wt.%) as internal

standard in a boron capillary and spun under the beam. The diffraction patterns were collected using a multi-analyzer stage equipped with nine analyzer crystals and nine detectors. The combined RIR-Rietveld method, which enables the quantitative phase analysis (QPA) and the calculation of both the crystalline and amorphous fractions [43] was performed by using the GSAS package [44] with the EXPGUI interface [45].

Samples (Fe,H)A800C-0min and (Fe,H)A600C-90min were characterized by measuring the N_2 adsorption–desorption isotherms at -196 °C (QuantachromeAutsorb 1 apparatus) after outgassing at 250 °C for 4 h under a N_2 flow. The specific surface area of the samples was calculated according to the Brunauer–Emmett–Teller (BET) method (S_{BET}) [26,46].

Scanning electron microscopy (SEM) observations of samples (Fe,H)A800C-0min and (Fe,H)A600C-90 min were carried out on a FE-SEM Ultra Plus (Zeiss, GmbH) microscope at 20 kV. Zeolites particles were deposited on a silicon surface from ethanol solutions and left dry in a vacuum chamber at 50°C overnight, before the observation the samples were sputter coated with gold (about 5 nm of gold were deposited by 208 HR sputter coater, Cressington Scientific Instruments Ltd, UK).

Transmission electron microscopy (TEM) observations of (Fe,H)A800C-0min and (Fe,H)A600C-90min samples were carried out with a TECNAI 20 G2: FEI COMPANY (CRYO-TEM-TOMOGRAPHY, Eindhoven) with a camera Eagle 2HS. The images were acquired at 200 kV; camera exposure time: 1 s; size 2048 x 2048. Zeolite particles were deposited by drop casting an ethanol solution on a formvar/carbon Cu grid (Agar Scientific Ltd, UK) and leaving evaporate overnight in a vacuum chamber at 50°C. For the histogram of the size distribution of small nanoparticles (<15 nm), a diameter of ca. 100 particles was measured. Large metallic particles (>50 nm) were observed in a number too low to attain a statistically meaningful size distribution, thus their shape and size will be discussed only in a qualitative way.

The ζ-potential curve of samples (Fe,H)A800C-0min and (Fe,H)A600C-90 min in deionized water was obtained measuring the electrophoretic mobility as a function of pH at 25 °C by means of

electrophoretic light scattering (ELS) (Zetasizer Nano-ZS, ZEN5600, Malvern Instruments, Worcestershire, UK). Suspensions were obtained after 2 min of sonication with an ultrasonic probe (100 W, 20 kHz, Sonoplus; Bandelin, Berlin, Germany); the pH of the suspension was adjusted by adding either 0.1 M HCl or 0.1 M NaOH.

Magnetic studies on both metal-ceramic nanocomposites were carried out at room temperature using a Lakeshore 720 vibrating sample magnetometer under a magnetic field ranging from -17 to 17 kOe.

2.4 Analytical determination

Simazine concentration in solution was analyzed with an Agilent 1200 Series HPLC apparatus (Wilmington U.S.A.), equipped with a DAD array and a Chem Station Agilent Software. A Macharey-Nagel Nucleosil 100-5 C18 column (stainless steel 250 x 4 mm) was utilized. The mobile phase, comprising a binary system of 65:35 acetonitrile: water, was pumped at 1 $mL \cdot min^{-1}$ flow in an isocratic mode. The detector was set at 220 nm and injection volume was 20 µL. The quantitative determination of simazine was performed elaborating its corresponding calibration curve between 0.15-20 µmol/L.

2.5 Adsorption experiments

Aqueous solutions with different simazine concentrations were contacted with the (Fe,H)A800C-0min and (Fe,H)A600C-90min samples in glass vials with Teflon caps at 25°C; the vessels were continuously stirred in an orbital shaker at 150 *rpm* until steady state conditions were approximated, which took about 24 h. Finally, the magnetic adsorbents (Fe,H)A800C-0min and (Fe,H)A600C-90min were separated from the liquid using an external magnet (VA03, UNIDISP s.r.l. Italy) and the liquid was analysed to evaluate simazine concentration, using HPLC. The amount of simazine adsorbed was calculated as the difference between its initial and final concentration in solution. Blanks of simazine in doubly distilled water were analysed in order to evaluate simazine stability and sorption on vials.

The following experimental factors were evaluated:

(a) *Effect of pH.* Magnetic adsorbents (Fe,H)A800C-0min and (Fe,H)A600C-90min were contacted with 10.0 µmol/L simazine solution at solid/liquid ratio (s/l) = 1/10,000 g/g. The pH of this solution was varied between 2 and 8, in steps of 0.5, by adding the proper amount of 0.01 or 0.10 mmol/L HCl or NaOH aqueous solution.

(b) *Adsorption time.* Kinetic studies were performed by contacting the magnetic adsorbents (Fe,H)A800C-0min and (Fe,H)A600C-90min with 20.0 µmol/L simazine solution, at S/L = 1/10,000 g/g and pH 6.5 and 3.0, respectively (pH of maximum simazine adsorption). The suspensions were stirred up to 48 h and successively subjected to the separation procedure described.

(c) *Sorption isotherm*. Magnetic adsorbents (Fe,H)A800C-0min and (Fe,H)A600C-90min were contacted with solutions having simazine concentration up to 20.0 µmol/Lat S/L = 1/10,000 g/g, T = 25 °C and pH = 6.5 or 3.0, respectively, for 24 h. The pH of each suspension was kept constant by adding proper amounts of 0.01 or 0.10 mmol/L HCl or NaOH solution.

2.6 Simazine removal by direct addition of the magnetic adsorbents.

A first group of experiments was performed as follows. Magnetic adsorbents (Fe,H)A800C-0min and (Fe,H)A600C-90min were contacted with 10.0 µmol/L simazine aqueous solutions at S/L ratio = 1/10,000 g/g and pH = 6.5 or 3.0, respectively, for 24 h. Subsequently, the suspensions were subjected to the solid-liquid magnetic separation and the resulting simazine concentration was determined. This same solution was again contacted with a fresh amount of the magnetic adsorbents (Fe,H)A800C-0min or (Fe,H)A600C-90minat the same S/L ratio and this procedure was iterated until the resulting simazine concentration went below 0.25 µmol/L.

A second group of the same type of experiments was performed by contacting the magnetic adsorbents (Fe,H)A800C-0min and (Fe,H)A600C-90min with 10.0 µmol/L simazine aqueous solution at S/L ratio = 1/1,000 g/g and at pH = 6.5 or 3.0, respectively, for 1.5 h.

3. Results

3.1 Chemical Composition

The chemical analysis of the $Fe^{2+}$and NH_4^+ exchanged samples of zeolite A, which after the thermal treatment under reducing atmosphere gave rise to magnetic adsorbents (Fe,H)A800C-0min and (Fe,H)A600C-90min, revealed what follows. Magnetic adsorbent (Fe,H)A800C-0min has Fe^{2+}, NH_4^+ and residual Na^+ contents of 2.33, 2.28 and 0.87meq/g, respectively, and magnetic adsorbent (Fe,H)A600C-90min 4.74, 0.44 and 0.30 meq/g, respectively. The weight percentage of Fe in the magnetic adsorbents (Fe,H)A800C-0minand (Fe,H)A600C-90min was calculated on the basis of the Fe^{2+} content of the parent $Fe^{2+}$and NH_4^+ exchanged samples of zeolite A, bearing in mind that the final products are completely dehydrated and deammoniated. They were 8.8 and 16.7 %, respectively. Magnetic adsorbent (Fe,H)A600C-90min has a weight percentage of Fe almost double of magnetic adsorbent (Fe,H)A800C-0min. This finding appears fully justified by the different cation exchange procedures followed for the two samples. Actually the zeolite sample which was transformed by the thermal treatment under reducing atmosphere in sample (Fe,H)A600C-90min, was subjected to eight exchange in the presence of the lone cation Fe^{2+}. The zeolite sample which was transformed by the thermal treatment under reducing atmosphere in sample (Fe,H)A800C-0min, was subjected to only two exchange with the contemporaneous presence of both cations $Fe^{2+}$and NH_4^+.

3.2 X Ray Diffraction

The XRD pattern of zeolite Na-A and Fe^{2+} and NH_4^+ exchanged zeolite A samples (not reported) suggested that cation exchange operations resulted in a partial distortion of the zeolite A framework, denoted by the depression of its diffraction peaks.

The results of the quantitative phase analysis (QPA) are reported in Table 1, and the observed and calculated patterns in Figures 2a and b.

In both samples the amorphous matrix represents almost the 90% of the sample (87.1 and 86.4 wt. % for (Fe,H)A600C-90min and (Fe,H)A800C-0min, respectively). In both cases it is possible to

recognize the precursor zeolite, even in the case of the (Fe,H)A600C-90min sample, the crystalline precursor is present in levels lower than 1%, indicating that the material is almost completely amorphous. Metallic Fe peaks were recorded in both patterns, although for (Fe,H)A800C-0min sample their intensities were very low. The QPA results indicate an amount of Fe^0 of 4.8 and 0.2 wt. %, for (Fe,H)A600C-90min and (Fe,H)A800C-0min, respectively. Large peaks referable to iron oxides were recovered in both samples: magnetite (Fe_3O_4) is present in both samples (7.1 and 5.4 wt. % for (Fe,H)A600C-90min and (Fe,H)A800C-0min, respectively) while wustite (FeO) was detected in low traces (0.2 wt. %) in sample (Fe,H)A600C-90min only. The absence of maghemite (γ-Fe_2O_3) in addition to magnetite, was established on the basis of the absence of peaks (210) and (211) of maghemite, that should be found at 6.33 and 6.96 ° 2θ, respectively, in this data collection[47]. Anyway, the presence of traces of maghemite cannot be ruled out since the peaks (210) and (211) could have very low intensities. In fact, due to low amount iron oxides in this mixture, even the main peaks or Fe_3O_4 are very weak.

3.3 Textural and Morphological Characterization

N_2 adsorption isotherms of prepared nanocomposites (not reported) are of type II, representative of either non-porous adsorbents or adsorbents having relatively large pores.

The adsorption isotherms were used to determine the values of specific surface area (S_{BET}), the total pore volume (V_{mp}) and micropore volume (V_{mp}) reported in Table 2.

The pore size distribution (PSD) curves (not reported) evidenced that the thermal collapse of the original microporous zeolite structure provoked the formation of mesopores with a diameter size spread in a range up to 50 nm while micropores are not more present, in both samples, Table 2. In addition, the followed preparation procedure caused the formation of a non-negligible fraction of macropores.

As reported by the SEM analysis, the treatments proposed here seemed to preserve the cubic shape of the basic unit of pristine zeolite A (Fig 3 A-C), despite of the thermal collapse of the original

microporous zeolite structure. Nevertheless, traces of the dramatic structural transformations, occurred during the thermal treatment under reducing atmosphere, may be found in the fact that the side length of the cube decreased and the angle smoothed. Actually the side of the cube-shaped microporous crystalline grains of the original zeolite A measures about 1.55 μm, while, on average, the side of the cube-shaped, amorphous, more compact, grains of sample (Fe,H)A800C-0min (Fig. 3 D) and (Fe,H)A600C-90min (Fig. 3 G) measures 1.1 and below 1 μm with rounded edges, respectively. More importantly the surfaces of the particle units are roughened upon the treatment. In the case of (Fe,H)A800C-0min (Fig.3 E-F) the surface presents interconnected pores with elongated formations, in the case of (Fe,H)A600C-90min (Fig 3 H-I) the surface presents more compact with globular clusters around 40 – 70 nm.

Figure 4A and B shows representative TEM images of samples treated, (Fe,H)A800C-0min and (Fe,H)A600C-90min, where clusters and nanoparticles of magnetite and metallic iron exhibit higher amplitude (mass/thickness) contrast with respect to the ceramic matrix in which are embedded, producing darker projections of their 3D shapes in the 2D image plane. In the case of (Fe,H)A800C-0min small nanoparticles of about 11 nm are formed and located mainly on the edges of the zeolite grains. Large aggregates with size over 200 nm can be also observed.

In the case of sample (Fe,H)A600C-90min (Figure 4B) large aggregates dominate the structure with a non-homogeneous surface structure. However, small nanoparticles with a size on average of 1.82 nm with and an asymmetric distribution can be observed.

3.4 ζ-potential curves

The ζ-potential of (Fe,H)A800C-0min and (Fe,H)A600C-90min nanocomposites, dispersed in ultrapure water, was determined at various pH (curves not reported). Both magnetic adsorbents are negatively charged in water at neutral pH, reaching the point of zero charge (PZC) at pH 3.7 and 5.6, respectively. This finding denotes that sample (Fe,H)A800C-0min exhibits an higher amount of acidic hydrogen sites than sample (Fe,H)A600C-90min.

3.5 Magnetic Characterization

The magnetic hysteresis loops of (Fe,H)A800C-0min (red symbols) and (Fe,H)A600C-90min (black symbols) are shown in Fig. 5. The magnetization values at the maximum applied field are M_s = 4.2emu/g and M_s = 12.3 emu/g, respectively; complete magnetic saturation is actually not achieved at 17 kOe, as expected from nanoparticulate systems. The magnetization loops are characterized by quite different coercive fields H_c (inset in Fig. 5).Similar results concerning M_s, H_c and the non-saturating character of magnetization curves of various Fe nanoparticles systems, obtained through different procedures, are reported in the literature [48,49].

3.6 Adsorption measurements

3.6.1 Effect of pH

Figure 6 reports the amount of simazine adsorbed on (Fe,H)A800C-0min and (Fe,H)A600C-90min sample as a function of pH. The two curves exhibit a sharp simazine adsorption peak of about 25,000 µmol/kg at largely different pH values such as 6.5 and 3.0, respectively. At different pH values simazine uptake by the two magnetic adsorbents drastically decreased. Thus, all the remaining experiments of simazine removal from waters by (Fe,H)A800C-0min and (Fe,H)A600C-90min samples, described in this study, were performed at the pH value of maximum simazine adsorption.

3.6.2 Kinetic and equilibrium features of the adsorption process

Figure 7 reports simazine uptake from water by (Fe,H)A800C-0min and (Fe,H)A600C-90min samples at pH 6.5 and 3.0, respectively, as a function of time (s/l ratio = 1/10,000 g/g). Simazine uptake on both magnetic adsorbents initially is quite rapid, then gradually slows down and finally, after about 24 h adsorption time, attains the equilibrium. Nevertheless adsorption on (Fe,H)A600C-90min sample appeared to proceed faster than on sample (Fe,H)A800C-0min. Such values of simazine uptake become similar for the two magnetic adsorbents only after 24 h have elapsed from the beginning of the adsorption process. On the basis of these considerations, the values of simazine

uptake or residual concentration in solution recorded at this time were considered as equilibrium values in the remaining of this work.

The two kinetic curves were analysed adopting both a pseudo first- and pseudo second-order kinetic model[50].The best model describing the sorption kinetics data was the pseudo second-order model whose linear form can be denoted as follows:

$$\frac{t}{q} = \frac{1}{k_2 \cdot q_e^2} - \frac{t}{q_e} \qquad \text{(E1)}$$

where q_e and q are the amount of herbicide sorbed (µmol/kg) at equilibrium and at time t, respectively, k_2 is the rate constant of adsorption (kg/(µmol·h)) and t is the time (h). The values of the model parameters are:

1) q_e = 30229 µmol/kg, $k_2 = 3.2 \cdot 10^{-5}$kg/(µmol·h) (r^2 = 0.999) for sample (Fe,H)A800C-0min);
2) q_e = 31389 µmol/kg, $k_2 = 1.52 \cdot 10^{-4}$kg(/µmol·h) (r^2= 0.999) for sample (Fe,H)A600C-90min.

The sorption isotherm of simazine on (Fe,H)A800C-0min and (Fe,H)A600C-90min samples is reported in Figure 8. These data are analyzed according to the Freundlich equation:

$$q_e = Kc^{1/N} \qquad \text{(E2)}$$

where q_e is defined as the amount of pesticide adsorbed (µmol/kg), c is the equilibrium concentration of pesticide in solution (µmol/L), K [(µmol/kg)/(µmol/L)$^{1/N}$] and N (dimensionless) are constants that give estimates of the adsorptive capacity and intensity, respectively [51].

The K and N values, obtained by the linearized form of Freundlich equation were 2269.9 [(µmol/kg)/(µmol/L)$^{1/N}$] and 0.95 (r^2>0.99) for (Fe,H)A800C-0minsample, and 1084.2 [(µmol/kg)/(µmol/L)$^{1/N}$] and 0.78 (r^2>0.99) for (Fe,H)A600C-90min sample. According to Giles et al. [51], the classification of the experimental adsorption isotherms was of S-type and subgroup 1.

The data of the adsorption isotherm were analyzed also according to the Langmuir model, but the obtained results (not reported) were decidedly unsatisfactory.

3.6.3 Simazine removal by iterative process

The results of the first group of experiments for an iterative process of simazine removal from water, performed by repeatedly contacting (Fe,H)A800C-0min and (Fe,H)A600C-90min samples with simazine aqueous solutions of 10 μmol/L initial concentration, at S/L ratio = 1/10,000 g/g and pH = 6.5 or 3.0, respectively, for 24 h are reported in Figure 9. These results evidence that this iterative process allows to bring simazine concentration below the law limit (0.05 mg/L ≈ 0.25 μmol/L) in 8-9 and 7-8 iterations using (Fe,H)A800C-0min and (Fe,H)A600C-90min sample, respectively as adsorbent.

The results of the second group of experiments for an iterative process of simazine removal from waters, performed by repeatedly contacting (Fe,H)A800C-0min and (Fe,H)A600C-90min samples with simazine aqueous solutions of 10 μmol/L initial concentration, at S/L ratio = 1/1,000 g/g and pH = 6.5 or 3.0, respectively, for 1.5 h are reported in Figure 10. These results evidence that this iterative process allows to bring simazine concentration below the law limit (0.05 mg/L ≈ 0.25 μmol/L) in 4-5 and 5-6 iterations using (Fe,H)A800C-0min and (Fe,H)A600C-90min sample, respectively, as adsorbent.

4. Discussion

The modalities of preparation of samples (Fe,H)A800C-0min and (Fe,H)A600C-90min need some consideration. In particular Fe^{2+} bearing exchange solutions were kept at about 7 °C and were Ar bubbled as the authors of ref. [38] found that it is the best way to avoid Fe^{2+} oxidation to Fe^{3+}. The occurrence of this phenomenon must be absolutely avoided during the exchange experiments, as trivalent iron would exchange a larger amount of monovalent cations, present in the zeolite framework, than divalent iron. Obviously, such an occurrence would result in a lower content of iron bearing phases in the final adsorbents, which could be detrimental for their magnetic properties. However, Fe^{2+} oxidation to Fe^{3+} occurs, at least partially, in the environment with about 50% relative humidity, where the zeolite samples were kept after the exchange experiments (see Experimental

section). Thus, this oxidation, once completed the exchange procedures, has no effect on the iron amount present in the zeolite framework. Moreover, it fully justifies the presence of Fe^{3+} cations in the zeolite framework prior to the thermal treatment under reducing atmosphere, which gives rise to the crystallization of Fe_3O_4 in samples (Fe,H)A800C-0min and (Fe,H)A600C-90min. The oxidation of Fe^{2+} to Fe^{3+} after the exchange experiment and prior to the thermal treatment under reducing atmosphere is confirmed by the color variations that the precursor zeolite undergoes in the various steps of the process. Actually zeolite Na-A and (NH_4-Na)-A is white, zeolite (Fe-NH_4-Na)-A as obtained just after Fe-exchange is green (color typical of hydrated Fe^{2+}), and zeolite (Fe-NH_4-Na)-A, after one day has elapsed from the end of the Fe-exchange, turns yellowish-brown (color typical of hydrated Fe^{3+}).

The patented process on which the production of the magnetic adsorbents (Fe,H)A800C-0min and (Fe,H)A600C-90min is based, proved to be very versatile [31-34]. Actually this process was found to be largely affected by a number of parameters. Among them, the framework type of the parent zeolite, the temperature and duration time of the thermal treatment and the modalities of cation exchange procedures are only the most evident. Thus, the two magnetic adsorbents, although obtained starting from the same precursor (zeolite A), were deliberately produced following different routes, which resulted into two largely different final products.

The *raison d'être* of the procedures adopted to prepare sample (Fe,H)A800C-0min are the following. The parent zeolite A was, firstly, NH_4^+ exchanged twice and, secondly, NH_4^+ and Fe^{2+} exchanged twice to introduce in the zeolite framework a large amount of NH_4^+ and a moderate amount of Fe^{2+}. During the subsequent thermal treatment under reducing atmosphere the large amount of NH_4^+ gives raise to the same amount of acidic hydrogen sites, through the evolution of gaseous ammonia and the moderate amount of $Fe^{2+}$to a moderate amount of magnetic phases [52,53]. Actually acidic hydrogen sites are known to exhibit a good affinity for the basic simazine molecule [25,26] and the moderate

amount of magnetic phases ensures a simple magnetic separation of the magnetic adsorbent from water.

The *raison d'être* of the procedures adopted to prepare sample (Fe,H)A600C-90min are the following. The parent zeolite A was, firstly, NH_4^+ exchanged ten times in order to leave in its framework a residual Na^+ content as low as possible. After these ten NH_4^+ exchange, zeolite A contains mainly NH_4^+, which is known to be easily exchanged by other cations.The easiness of Fe^{2+} exchange for NH_4^+ (iterated eight times) allows to enhance as much as possible the amount of Fe^{2+} finally present in the framework of zeolite A. Such a large Fe^{2+} amount gives rise, during the subsequent thermal treatment under reducing atmosphere, in a large amount of magnetic phases which ensures a strong magnetic response of the adsorbent. Moreover, the residual NH_4^+ content of zeolite A gives rise to an equivalent amount of acidic hydrogen sites through the evolution of gaseous ammonia [52,53].

In both nanocomposites (Fe,H)A800C-0min and (Fe,H)A600C-90min, Fe^0 and Fe_3O_4 nanoparticles are located close to the acidic hydrogen sites generated by the NH_3 evolution, which could result in their, at least, partial dissolution. Such dissolution appears to occur to a very limited extent, if any, as Fe^0 and Fe_3O_4 nanoparticles are sufficiently protected by the amorphous silica-alumina ceramic matrix in which they are embedded. Moreover, one may object that, before preparing nanocomposites by simultaneously NH_4^+ and Fe^{2+} exchanging zeolite A, it would be wise firstly prepare and test adsorbents by separately exchanging zeolite A with NH_4^+ or Fe^{2+}. It was not done as:

1) adsorbents prepared without Fe^{2+} would not be magnetic;
2) nanocomposites prepared by exchanging zeolite A only withFe^{2+} were produced for the DNA separation in ref. [35]. These adsorbents were preliminarily tested in simazine removal from water and obtained results (not reported) were largely worse than those of this work.

Regarding temperature and duration of thermal treatment, it is well known that the extent to which the Fe^{2+} reduction occurs and the dimension of metallic Fe or magnetite nanoparticles is the larger, the higher the temperature and the longer the duration time [31,32].Thus, two largely different thermal

treatments, both concerning temperature and duration time, were selected and attributed to the two different $Fe^{2+}$and NH_4^+ exchanged zeolite A samples, in order to obtain two magnetic adsorbent samples exhibiting largely different features. In particular, the shortest possible duration time (0 min, namely the furnace was switched off as soon as 800 °C were attained) was coupled with an higher temperature (800 °C), and a long duration time (90 min) with a lower temperature (600 °C).

The obtained results essentially matched all the previous considerations formulated in selecting the modalities of cation exchange and thermal treatment, to design the features of the magnetic adsorbents which are the final product of the process. Specifically, it was found that:

1) Magnetic adsorbent (Fe,H)A800C-0min has a far higher amount of acidic hydrogen sites (2.28 meq/g) than magnetic adsorbent (Fe,H)A600C-90min (0.44 meq/g) (these values were calculated on Fe^{2+} and NH_4^+ exchanged zeolite A before the thermal treatment under reducing atmosphere).The high amount of acidic hydrogen sites is confirmed by the low value of pH (3.7) at which the magnetic adsorbent (Fe,H)A800C-0min exhibits zero charge.
2) Magnetic adsorbent (Fe,H)A600C-90min exhibits an amount of magnetic phases (magnetite = 7.1 and metallic Fe = 4.8 wt. %) far higher than magnetic adsorbent (Fe,H)A800C-0min (magnetite = 5.4 and metallic Fe = 0.2 wt. %).Moreover, magnetic adsorbent (Fe,H)A600C-90min exhibits a moderate, lower than magnetic adsorbent (Fe,H)A800C-0min,amount of acidic hydrogen sites. This finding is confirmed by the moderately acidic pH (5.6) of zero charge.
3) Magnetic adsorbent (Fe,H)A800C-0min exhibits an high number of small magnetite and metallic iron nanoparticles with an average dimension of about 11 nm, together with few large particles with size over 200 nm, whereas magnetic adsorbent (Fe,H)A600C-90min exhibits a smaller (than (Fe,H)A800C-0min sample) number of small magnetite and metallic iron nanoparticles with an average dimension of 1.82 nm, together with an higher (than (Fe,H)A800C-0min sample) number of large particles with size over 200 nm.

4) The different amount of magnetic phases present in the final products and their different morphology results in a strongly different magnetic behaviour at room temperature, as shown in Fig. 4. Magnetic adsorbent (Fe,H)A600C-90min exhibits a magnetic response far stronger than magnetic adsorbent (Fe,H)A800C-0min, as expected from the estimated amounts of ferro/ferrimagnetic phases present. The magnetic adsorbent (Fe,H)A800C-0min, particularly rich in magnetite, has a coercivity typical of Fe_3O_4 nanoparticles (≅ 50 Oe), while the coercive field of magnetic adsorbent (Fe,H)A600C-90min (H_c≅ 380 Oe) is fully compatible with the presence of higher-anisotropy nanoparticles of metallic Fe. In both materials, the high-field magnetization appears to be perfectly consistent with an easy and fast magnetic separation [54]. Nevertheless, it must be noted that the stronger magnetic response of magnetic adsorbent (Fe,H)A600C-90min than magnetic adsorbent (Fe,H)A800C-0min,results in the fact that the former adsorbent is separated more promptly from the water containing simazine than the latter.

The previous considerations account for the fact that the two magnetic adsorbents (Fe,H)A800C-0min and (Fe,H)A600C-90min largely differ from each other. Despite of it, they exhibit similar, very good performances, in the removal of simazine from water. In particular, the examination of Fig. 8 allows the following considerations. This figure reports the isotherms of simazine adsorption from water on the two magnetic adsorbents (Fe,H)A800C-0min and (Fe,H)A600C-90min, zeolite H-Y and micro- meso-porous silica sample SiO_2(II)400 [25,26]. All these isotherms exhibit an adsorption plateau of about 12000 (zeolite H-Y), 30000 (magnetic adsorbents (Fe,H)A800C-0min and (Fe,H)A600C-90min) and 40000 µmol/L (silica sample SiO_2(II)400). This fact could infer the superficial consideration that magnetic adsorbents (Fe,H)A800C-0min and (Fe,H)A600C-90min works better than zeolite H-Y but worse than silica sample SiO_2(II)400. It is not so on account of what follows. The concentration levels at which the various agrochemicals are usually present in water bodies are usually lower than 10 µmol/L [13,14]. Moreover, the law limit is 0.05 mg/L[3] ≈ 0.25

μmol/L. Thus, an adsorbent, viable for practical applications, to be used for simazine removal from water, must bring simazine concentration from not more than 9-10 μmol/L to below 0.25 μmol/L. In such simazine concentration range the adsorption isotherm of magnetic adsorbents (Fe,H)A800C-0min and (Fe,H)A600C-90min lies far above than those of silica sample SiO_2(II)400 and zeolite H-Y, thus certifying their higher efficiency in the simazine adsorption process. In addition, in refs. [25,55] supplementary data concerning simazine adsorption on other adsorbents are reported, showing that the magnetic adsorbents of this work exhibit far better performances in simazine removal from water.

The good efficiency of magnetic adsorbents (Fe,H)A800C-0min and (Fe,H)A600C-90min in the simazine removal from water is confirmed even by the kinetic runs (Fig. 7) and by the results of the iterative process of simazine removal from water (Figs. 9 and 10). Regarding kinetic runs, a steady state is attained in about one day, but about 65 and 90 % of simazine final uptake is recorded in about 1.5-2 h, respectively. Regarding the iterative process, Fig. 9 reports that 7-8 iterations (at S/L = 1/10,000 g/g and 24 h contact time) are sufficient to bring simazine concentration below the law limit (0.25 μmol/L), whereas Fig. 10 that 5-6 iterations (at S/L = 1/1,000 g/g and 1.5 h contact time) are sufficient to attain the same goal. In practice, these results mean that the simazine amount present in 1 m^3 of water, at the concentration level usually present in the water bodies, can be brought below the law limit (0.05 mg/L ≈ 0.25 μmol/L) by:

1) using 0.7-0.8 kg of magnetic adsorbents (Fe,H)A800C-0min or (Fe,H)A600C-90min in 7-8 days;
2) using 5-6 kg of magnetic adsorbents (Fe,H)A800C-0min or (Fe,H)A600C-90min in 9-10 h.

A last point deserves to be discussed. Both curves reporting the simazine uptake from water as a function of pH, exhibit a sharp maximum slightly higher than 25,000 μmol/kg. However this maximum occurs at largely different pH values (6.5 and 3.0, magnetic adsorbents (Fe,H)A800C-0min and (Fe,H)A600C-90min, respectively, Fig. 6). This fact appears an evidence that samples

(Fe,H)A800C-0min and (Fe,H)A600C-90min adsorb simazine following largely different mechanisms. The interpretation of this point is facilitated by our previous study. Regarding (Fe,H)A800C-0min, its pH of maximum simazine adsorption is 6.5, as zeolite H-Y does [25]. Moreover, these two adsorbents have in common also the large number of acidic hydrogen sites derived from the large amount of NH_4^+ present in the framework of zeolite A or Y. Thus, it appears more than likely that magnetic adsorbent (Fe,H)A800C-0min and zeolite H-Y follows the same mechanism of simazine adsorption. In particular, the Lewis acidic centers of these two adsorbents, once soaked in water, turn into Brønsted acidic centers [52,53]. In turn simazine behaves as a base because of the electron lone pairs located in the lateral chains of the molecule. Thus, simazine uptake by magnetic adsorbents (Fe,H)A800C-0min and zeolite H-Y can be considered as involving a typical acid-base reaction. These interactions occur most favorably at a pH where the following two phenomena balance each other as:

1) At alkaline pH, hydroxyl anions neutralize the acid sites of the two adsorbents, forming Si-(O^-)-Al groups, being OH^- a base stronger than simazine;
2) At acidic pH, hydronium cations form substituted NH_4^+ species by reacting with the nitrogen lone pair electrons of simazine.

Additionally, this interpretation is strongly supported by the decidedly acidic pH of zero charge (3.7) of the magnetic adsorbent (Fe,H)A800C-0min. Thus, its surface, at the pH of maximum simazine adsorption (6.5), is negatively charged. These negatively charged sites interact with the fraction of simazine molecules which, at this same pH, turns out protonated. As adsorption of protonated simazine molecules on the surface of the magnetic adsorbent (Fe,H)A800C-0min goes on and tend to depress its equilibrium concentration, further protonated simazine molecules arise from the reaction of simazine with hydronium cations.

Regarding magnetic adsorbent (Fe,H)A600C-90min, its pH of maximum simazine adsorption is 3.0. In a previous study regarding sorption of simazine on mesoporous metal oxides [55], it was reported

that the maximum sorption of simazine on Fe_2O_3 occurred at pH 3.5. The fact that the pH of maximum simazine adsorption on mesoporous Fe_2O_3 and sample (Fe,H)A600C-90min (containing an higher Fe_3O_4 amount) are very similar suggests that, when water containing simazine is contacted with such magnetic adsorbent, simazine molecule prevailingly interacts with the magnetite present therein. In such interactions hydronium cations play a crucial role. Such role could very likely be the formation of intermolecular hydrogen bond in the simazine-magnetite, or possibly even simazine-silica, contact layer. Such formation was already recorded in the *Escherichia Coli* DNA adsorption on magnetic metal-ceramic adsorbents of the same family of those studied in this work [35,56-57]. This fact does not appear a mere coincidence as the surface of adsorbents are similar in both cases and *Escherichia Coli* DNA molecule exhibits the electron lone pairs of its nitrogen bearing bases similar to the electron lone pairs located in the lateral chains of the simazine molecule. Moreover, this interpretation is strongly supported by the moderately acidic pH of zero charge (5.6) of the magnetic adsorbent (Fe,H)A600C-90min. Thus, its surface, at the pH of maximum simazine adsorption (3.0), is positively charged because of the hydronium cations adsorbed there. Obviously, such hydronium cations will form hydrogen bonds between the surface of the adsorbent and the molecules of simazine.

What appears surprising is that two largely different adsorbents which adsorb simazine through two largely different mechanisms, exhibit both similar and very good performances in the removal of simazine from water. The fact that the two magnetic adsorbents have two largely different pH of maximum adsorption could be useful from the practical point of view, if one bears in mind the results of ref. [29]. This work, which studies the differences of the simazine adsorption process from model and natural water on zeolite H-Y and the mesoporous silica SiO_2(II)400, concludes that the nature of the water in which the simazine is present does not affect very much the simazine adsorption process, provided the pH of the natural water does not differ very much from the pH of maximum simazine adsorption. Thus, it appears proper to remove simazine from water by adsorption from a natural water

using an adsorbent which exhibits a pH of maximum adsorption as close as possible to the one of the natural water.

Finally, the regeneration of the exhausted simazine-bearing adsorbents does not appear to be a problem on the basis of what follows. It is reported in the literature that, whenever the adsorbate exhibits a low thermal stability and the adsorbent a good thermal and chemical stability, thermal regeneration of the exhausted adsorbents appears to be fast, simple and cheap [58,59]. Actually it avoids the tedious elution steps of exhausted adsorbents and the consequent destruction or immobilization of the polluting adsorbate. This is just the case of the regeneration of the simazine bearing, exhausted (Fe,H)A800C-0min and (Fe,H)A600C-90min magnetic adsorbents as:

1) the thermal analysis of simazine shows a sharp endothermic peak at about 250 °C that can be reasonably ascribed to its thermal decomposition [25];
2) at temperatures up to 500 °C, under inert or reducing atmosphere, (Fe,H)A800C-0min and (Fe,H)A600C-90min magnetic adsorbents exhibit high thermal and chemical stability owing to the low atomic mobility and absence of chemical reactions, respectively.

Thus, a no more than 5 min thermal treatment at about 300 °C, under inert or reducing atmosphere, would surely fulfill the goal of an efficient and cheap regeneration of the adsorbents. Moreover, the outlet regenerating gaseous stream could be mixed with air, thus giving raise to the combustion of the molecules deriving from simazine decomposition. In this way the agrochemical simazine would be destroyed and mostly transformed into a small amount of carbon dioxide, molecular nitrogen and hydrochloric acid released in the atmosphere.

5. Conclusion

The results of this work show that the use of the metal-ceramic nanocomposites produced through the patented process of thermal transformation of cation exchanged zeolites under reducing

atmosphere [31,32], exhibit potential for practical application in the removal of agrochemicals from water. This conclusion is based on:

1) The efficiency of the magnetic adsorbents which allows to bring simazine concentration below the Italian law limit (0.05 mg/L).
2) The possibility of magnetically drive the adsorbents because of their significant magnetic response.
3) The intrinsic simplicity of the process and of the related operations. Actually, it is sufficient to use a large basin where the simazine bearing water and the magnetic adsorbent come into contact, and which, subsequently, will be magnetically separated from the water.
4) The simple and cheap regeneration of the exhausted adsorbent by a few minutes' thermal treatment at about 300 °C under inert or reducing atmosphere. Moreover, such regeneration involves also simazine destruction by combustion.
5) The molecules of the various agrochemicals do not differ very much from each other. Thus, it appears likely that the very good results obtained in simazine removal from water by adsorption on the family of magnetic adsorbents described in this work and their subsequent regeneration will not differ very much from the results that can be obtained when other agrochemicals should be removed from water.

NOTES

The authors declare no competing financial interest

Acknowledgements: The authors would like to thank ALFED S.P.A. for the kind financial contribution. Dr. Carlotta Giacobbe of ID22 Beamline@ESRF, Grenoble, is acknowledged for data collections. The authors would like to sincerely express their appreciation to Prof. Dianna Pickens

Centro Linguistico di Ateneo (CLA) Università degli Studi di Napoli "Federico II" for the careful editing of the manuscript.

References

1) B.Srivastava, V.Jhelum, D.D.Basu, P.K. Patanjali, Adsorbents for pesticide uptake from contaminated water: A review, J. Sci. Ind. Res. 68 (2009)839-850.
2) A.M.Derylo-Marczewska, A. Blachnio, W.Marczewski, B. Tarasiuk, Adsorption of selected herbicides from aqueous solutions on activated carbon, J. Therm. Anal. Calorim. 101 (2010) 785-794.
3) P. Chigombe, B. Saha, R.J. Wakeman, Sorption of atrazine on conventional and surface modified activated carbons, J. Colloid Interface Sci.302 (2006) 408-416.
4) L. Damjanovic, V. Rakic, V. Rac, D. Stosic, A. Aurox, The investigation of phenol removal from aqueous solutions by zeolite as solid adsorbents, J. Hazard. Mater.184 (2010) 477-484.
5) J. Ellis, W. Korth, Removal of geosmin and methylisoborneol from drinking water by adsorption on ultrastable zeolite-Y, Water Res. 4 (1993)535-539.

6) W.T. Tsai, K.J. Hsien, H. Hsu, Adsorption of organic compounds from aqueous solution onto the synthesized zeolite, J. Hazard. Mater.161 (2009) 635-641.

7) S. Salvestrini, P. Sagliano, P. Iovino, S. Capasso, C. Colella, Atrazine adsorption by acid-activated zeolite-rich tuffs, Appl. Clay Sci.49 (2010) 330-335.

8) M. Cruz-Guzman, R. Celis, M. Carmen Hermosin, W.C. Koskinen, J. Cornejo, Adsorption of pesticides from water by functionalized organobentonites, J. Agric. Food Chem.53 (2005) 7502-7511.

9) M.V. Shankar, K.K. Cheralathan, B. Arabindoo, M. Palanichamy, V. Murugesan, Enhanced photocatalytic activity for the destruction of monocrotophos pesticide by TiO_2-Hβ, J. Mol. Catal. A: Chem.223 (2004) 195-200.

10) M.V. Shankar, S. Anandan, N. Venkatachalam, B. Arabindoo, V. Murugesan, Fine route for an efficient removal of 2,4-dichlorophenoxyacetic (2,4-D) by zeolite supported TiO_2,Chemosphere63 (2006) 1014-1021.

11) J. Lemic, D. Kovacevic, M. Tomasevic-Canovic, D. Kovacevic, T. Stanic, R. Pfend, Removal of atrazine, lindane and diazinone from water by organo-zeolites, Water Res.40 (2006) 1079-1085.

12) M. Sprynskyy, T. Ligor, B. Buszewski, Clinoptilolite study of lindane and aldrin sorption processes from water solution, J. Hazard. Mater.151 (2008) 570-577.

13) D.L.Carlson, K.D. Than, A.Lynn Roberts, Acid- and base-catalyzed hydrolysis of chloroacetamide herbicides,J. Agric. Food Chem.54 (2006) 4740-4750.

14) K. Ignatowicz-Owsieniuk, I. Skoczko, Dependence of sorption of phenoxyacetic herbicides on their physico-chemical properties, Pol. J. Environ. Stud.11 (2002) 339-344.

15) S.S. Chen, S.J. Taylor, L.A. Mulford, Influences of molecular weight, molecular size, flux, and recovery for aromatic pesticides removal by nano filtration membranes, Desalination 160 (2004) 103-111.

16) S. Wang, Y. Peng, Natural zeolites as effective adsorbents in water and wastewater treatment, Chem. Eng. J.156 (2010) 11-24.

17) B. Paul, D. Yang, X. Yang, X. Ke, R. Frost, H. Zhu, Adsorption of the herbicide simazine on moderately acid-activated beidellite, Appl. Clay Sci.49 (2010)80-83.

18) M. Mahalakashmi, S. Vishnu Priya, B. Arabindoo, M. Palanichamy, V. Murugesan, Photocatalytic degradation of aqueous propoxur solution using TiO_2 and Hβ zeolite-supported TiO_2, J. Hazard. Mater.161 (2009) 336-343.

19) V.Albino, R. Cioffi, M. Pansini, C. Colella, Disposal of lead-containing zeolite sludges in cement matrix, Env. Techol.16 (1995) 147-165.

20) C. Colella, M. de' Gennaro, A. Langella, M. Pansini, Cadmium removal from wastewater using natural zeolites, Natural Zeolites 93, D. W. Ming and F. A. Mumpton, eds., Int. Comm. Natural Zeolites (1995) 377-384.

21) R. Cioffi, M. Pansini, D. Caputo, C. Colella, Evaluation of cement-based solidified materialsencapsulating Cd-exchanged natural zeolites, Env. Technol.17 (1996) 1215-1224.

22) M. Pansini, C.Colella, Dynamic data on lead uptake from water by chabazite, Desalination78 (1990) 287-295.

23) M. Pansini, C. Colella, Lead pollution control by zeolite, Eng. Mat. 2 (1990) 623-630.

24) C. Colella, M. Pansini, Lead removal from wastewater using chabazite tuff. In W. H. Flank & T. E. Whyte Eds.,"Perspectives in Molecular Sieve Science", ACS Symp.368 (1988) 500-511.

25) F. Sannino, S.Ruocco, A. Marocco, S. Esposito, M. Pansini, Cyclic process of simazine removal from waters by adsorption on zeolite H-Y and its regeneration by thermal treatment, J. Hazard. Mat. 229-230 (2012) 354-360.

26) F. Sannino, S. Ruocco, A. Marocco, S. Esposito, M. Pansini, Simazine removal from waters by adorption on porous silica taylored by sol-gel technique, Microporous Mesoporous. Mater.180 (2013) 178-186.

27) S. Esposito, F. Sannino, M. Pansini, B. Bonelli, E. Garrone, Modes of interaction of simazine with the surface of model amorphous silicas in water, J. Phys. Chem. C,117 (2013) 11203-11210.

28) F. Sannino, M. Pansini, A. Marocco, B. Bonelli, E. Garrone, S. Esposito, The role of outer surface/inner bulk Brønsted acidic sites in the adsorption of a large basic molecule, Phys. Chem. Chem. Phys. 17 (2015) 28950-28957.

29) F. Sannino, A. Marocco, E. Garrone, S. Esposito, M. Pansini, Adsorption of simazine on zeolite HY and sol–gel technique manufactured porous silica: A comparative study in model and natural waters, J. Env. Sc. & Heal. Part B50 (2015)777-787.

30) S. Esposito, E. Garrone, A. Marocco, M. Pansini, P. Martinelli, F. Sannino, Application of highly porous materials for simazine removal from aqueous solutions, Env. Tech. 372(2016) 2428-2434.

31) S. Esposito, A. Marocco, B. Bonelli, M. Pansini, Produzione di Materiali Compositi Metallo-Ceramici Nano Strutturati da Precursori Zeolitici. Brevetto Italiano, MI**2014**A000522.

32) S. Esposito, A. Marocco, B. Bonelli, M. Pansini, PCT international application published under Number WO**2015**/145230 A1.

33) A. Marocco, G. Dell'Agli, S.Esposito, M. Pansini, Metal-ceramic composite materials from zeolite precursor,Sol. St. Sc. 14 (2012) 394-400.

34) S. Ronchetti, E.A. Turcato, A. Delmastro, S. Esposito, C. Ferone, M. Pansini, B. Onida, D. Mazza, Study of the thermal transformations of Co- and Fe-exchanged zeolites A and X by"in situ" XRD under reducing atmosphere, Materials Research Bulletin45 (2010) 744–750

35) M. Pansini, G. Dell'Agli, A.Marocco, P.A. Netti, E. Battista, V. Lettera, P. Vergara, P. Allia, B. Bonelli, P. Tiberto, G. Barrera, G. Alberto, G. Martra, R. Arletti, S. Esposito, Preparation and characterization of magnetic and porous metal-ceramic nanocomposites from a zeolite precursor and their application for DNA separation, J. Biomed. Nanotechnol.13 (2017) 337-348.

36) A. Marocco, G. Dell'Agli, S. Esposito, M. Pansini, Parameters expediting the thermal conversion of Ba-exchanged zeolite A in monoclinic celsian, Advances in Materials Science and Engineering, 2010, Article ID 683429, 8 pages, doi:10.1155/2010/683429.

37) A. Marocco, G. Dell'Agli, S. Esposito, M. Pansini, The role of the residual Na^+ and Li^+ on thermal transformations of Ba-exchanged zeolite A, Solid State Sciences,13 (2011) 1143-1151.

38) C. Weidentaler, B. Zibrovius, J. Schimanke, Y. Mao, B. Mienert, E. Bill, W. Schmidt, Oxidation behaviour of ferrous cations during ion exchange into zeolites under atmospheric conditions, Microporous Mesoporous. Mater. 84 (2005) 302-317.

39) C. Ferone, B. Liguori, A. Marocco, S. Anaclerio, M. Pansini, C. Colella, Monoclinic (Ba, Sr)-celsian by thermal treatment of (Ba, Sr)-exchanged zeolite A, Microporous Mesoporous. Mater. 134 (2010) 65-71.

40) G. Dell'Agli, L. Spiridigliozzi, A. Marocco, G. Accardo, C. Ferone, R. Cioffi, Effect of the mineralizer solution in the hydrothermal synthesis of gadolinium-doped (10% mol Gd) ceria nanopowders, J.Appl. Biomater. Funct. Mater. 14 (2016) 189-196.

41) A. Marocco, G. Dell'Agli, B. Liguori, M. Pansini, Sintering behaviour of celsian based ceramics obtained from the thermal conversion of (Ba, Sr)-exchanged zeolite A, J. Eur. Ceram. Soc.31 (2011) 1965-1973.

42) S. Esposito, A. Marocco, G. Dell'Agli, B. de Gennaro, M. Pansini, Relationships between the water content of zeolites and their cation population, Microporous Mesoporous. Mater.202 (2015) 36-43.

43) A. F. Gualtieri, E. Mazzucato, P. Venturelli, A. Viani, P. Zannini, L. Petras, X-ray powder diffraction quantitative analysis performed in situ at high temperature: application to the determination of NiO in ceramic pigments, J. Appl. Crystallogr.32 (1999)808-813.

44) A.C. Larson, R.B. Von Dreele, General Structure Analysis System ″GSAS″; Los Alamos National Laboratory Report; Los Alamos, LAUR,1994**,** 86-748.

45) B. H. Toby, EXPGUI, a Graphical User Interface for GSAS., J. Appl. Crystallogr. 34 (2001) 210−213.

46) F. Rouquerol, J. Rouquerol, K. Sing, Adsorption by Powders and Porous Solids: Principles Methodology and Application, Academic Press, London, 1999.

47) W. Kim, C.-Y. Suh, S.-W. Cho, K.-M. Roh, H. Kwon, K. Song, I.-J. Shon, A new method for the identification and quantification of magnetite–maghemite mixture using conventional X-ray diffraction technique, Talanta, 94 (2012) 348-352.

48) J.L. Wilson, P. Poddar, N.A. Frey, H. Srikant, K. Mohomed, J.P. Harmon, S. Kotha, J. Wachsmith, Synthesis and magnetic properties of polymer nanocomposites with embedded iron nanoparticles, J. Appl. Phys., 95 (2004) 1439-1443.

49) M. Bhaumik, H.J. Choi, R.I. McCrindle, A. Moity, Composite nanofibers prepared from metallic iron nanoparticles and polyaniline: High performance for water treatment applications, J. Coll. Interf. Sc., 425 (2014) 75-82.

50) M. Ozacar, I.A. Sengil, A two-stage batch adsorbent design for methylene blue removal to minimize contact time, J. Environ. Manage.80 (2006) 372-379.

51) C.H. Giles, D. Smith, A. Huitson, A general treatment and classification of the solute adsorption isotherms, I. Theoret. J. Colloid Interface Sci.47 (1974) 755-765.

52) D.W. Breck, Zeolite Molecular Sieves: Structure, Chemistry and Uses, Wiley, New York, 1974.

53) F.G. Dwyer, An Introduction to Molecular Sieves Zeolites, J. Wiley and Sons, Chichester, UK, 1988.

54) R.K.Singh, T. H. Kim, K.D. Patel, J. C. Knowles, H.W. Kim, Biocompatible magnetite nanoparticles with varying silica coating layer for use in biomedicine: physicochemical and magnetic properties, and cellular compatibility, J. Biomed. Mater. Res. A 100A, 7 (2012) 1734-1742.

55) V. Addorisio, D. Pirozzi, S. Esposito, F.Sannino, Decontamination of waters polluted with simazine by sorption on mesoporous metal oxides, Journal of Hazard. Mater. 196 (2011) 242-247.

56) K. A. Melzak, C.S. Sherwood, R.F.B., Turner,C.A. Haynes, Driving Forces for DNA adsorption to silica in perchlorate solution, J. Colloid Interface Sci.181 (1996) 635-644.

57) X.Li, J. Zhang, H.Gu, Adsorption and desorption behaviors of DNA with magnetic mesoporous nanoparticles, Langmuir 27 (2011) 6099-6106.

58) L. R. Widger, M. Combs, A. R. Lohe, C. A. Lippert, J.G. Thomson, K. Lin, Selective removal of nitrosamines from a model amine carbon-capture water wash using low-cost activated carbon sorbents, Env. Sc. Technol. 51 (2017) 10913-10922.

59) K. T. Wong, N. C. Eu, S. Ibrahim, H. Kim, Y. Yon, M. Jang, Recyclable magnetite-loaded palm shell-waste based activated carbon for the effective removal of methylene blue from aqueous solution, Journal of Cleaner Production 115 (2016) 337-342.

Caption to Figures and Schemes

Scheme 1. Structure of simazine [2-chloro-4,6-bis(ethylamino)-1,3,5-triazine].

Figure 1. Sequence of the operations performed in the preparation of magnetic adsorbents (Fe,H)A600C-90min and b) (Fe,H)A800C-0min

Figure 2. Observed (green crosses) and calculated (red line) pattern after QPA analyses on sample a) (Fe,H)A600C-90min and b) (Fe,H)A800C-0min. The differences curve is reported in purple. Tick marks are relative to the different phases: black: LTA; red: magnetite; blue: Al_2O_3 standard; green: metallic Fe; yellow: wustite.

Figure 3. SEM representative images of parent zeolite A (A-B-C) showing the cubic shape of the

pristine material, (Fe,H)A800C-0min sample (D-E-F) and (Fe,H)A600C-90min (G-H-I).

Figure 4. Representative TEM images of (A) sample FeA800C-0min; an overall view and insets of portion of the composite with small clustered nanoparticles dispersed in/on the ceramic matrix. (3A, right) particle size distribution of small nanoparticles centered at 11.13 nm. (B) sample (Fe,H)A600C-90min; an overall view and insets of portion of the composite with small clustered nanoparticles dispersed in/on the ceramic matrix. (3B, right) particle size distribution of small nanoparticles centered at 1.82 nm.

Figure 5. Room-temperature magnetic hysteresis loops of (Fe,H)A800C-0min (red symbols) and (Fe,H)A600C-90min (black symbols); inset: low-field region.

Figure 6. Simazine adsorbed on (Fe,H)A800C-0min (full circles) and (Fe,H)A600C-90min (empty circles) samples from a 10 µmol/L simazine solution at s/l ratio = 1/10,000 g/g, after a contact of 24 h, as a function of pH.

Figure 7. Simazine uptake from waters by (Fe,H)A800C-0min (full circles) and (Fe,H)A600C-90min (empty circles) samples at pH 6.5 and 3.0, respectively, from a 20 µmol/L simazine solution, as a function of time (s/l ratio = 1/10,000 g/g).

Figure 8.Sorption isotherm of simazine on (Fe,H)A800C-0min (full circles), (Fe,H)A600C-90min (empty circles), zeolite HY(full triangle), and SiO2(II)400 (full square) samples.

Figure 9. Iterative process of simazine removal from waters, performed by repeatedly contacting (Fe,H)A800C-0min (full circles) and (Fe,H)A600C-90min (empty circles) samples with simazine

aqueous solutions of 10 μmol/L initial concentration, at s/l ratio = 1/10,000 g/g, for 24 h, and pH 6.5 and 3.0, respectively. Dotted line indicates the law limit <0.25 μmol/L.

Figure 10. Iterative process of simazine removal from waters, performed by repeatedly contacting (Fe,H)A800C-0min (full circles) and (Fe,H)A600C-90min (full squares)samples with simazine aqueous solutions of 10 μmol/L initial concentration, at s/l ratio = 1/1,000 g/g, for 1.5 h, and pH 6.5 and 3.0, respectively. Dotted line indicates the law limit <0.25 μm/L.

TABLES

Table 1. Results of Quantitative Phase analysis performed with Rietveld method. All the data are reported in wt. %

Sample	LTA_Fe %)	Magnetite%	Wustite %	Fe%	amorphous phase%
(Fe,H)A600C-90min	0.8(3)	7.1(3)	0.2(1)	4.8(1)	87.1
(Fe,H)A800C-0min	8.0(2)	5.4(1)		0.2(1)	86.4

Table 2. Specific surface area (S_{BET}), total pore volume (V_p) and micropore volume (V_{mp})

Sample	S_{BET} (m^2/g)	V_p (cm^3/g)	V_{mp} (cm^3/g) [a]	Pore diameter (nm)
(Fe,H)A600C-90min	28	0.15	/*	5-50
(Fe,H)A800C-0min	19	0.13	/*	5-50

[a]As obtained according to the t-plot method

Scheme 1

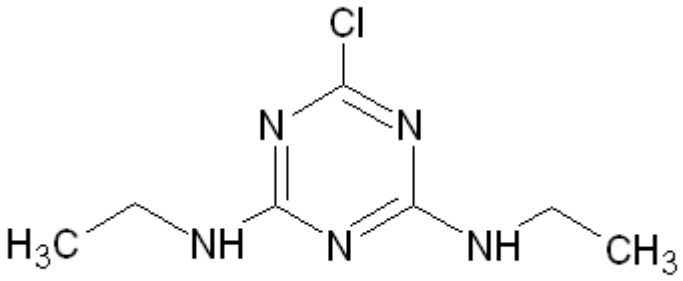

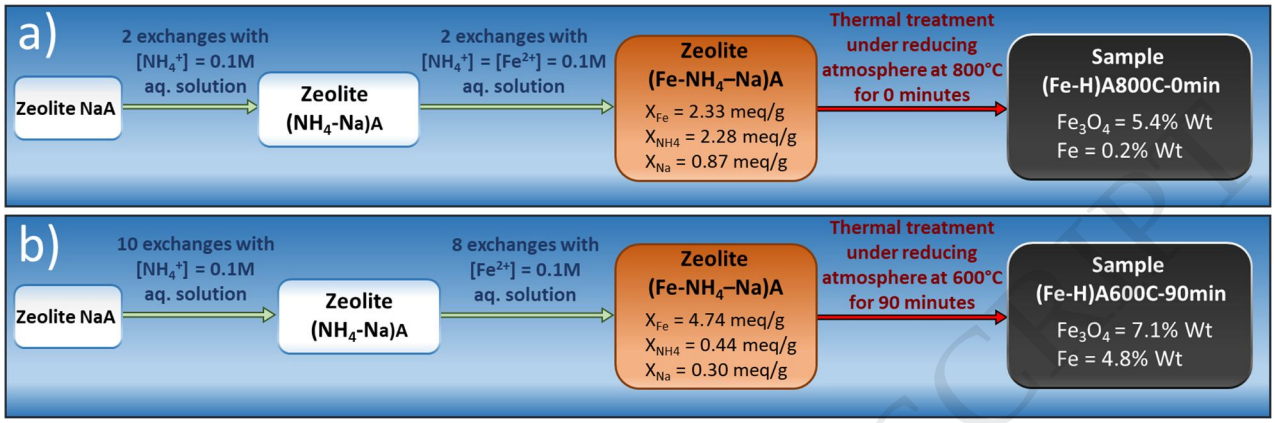

Figure 1

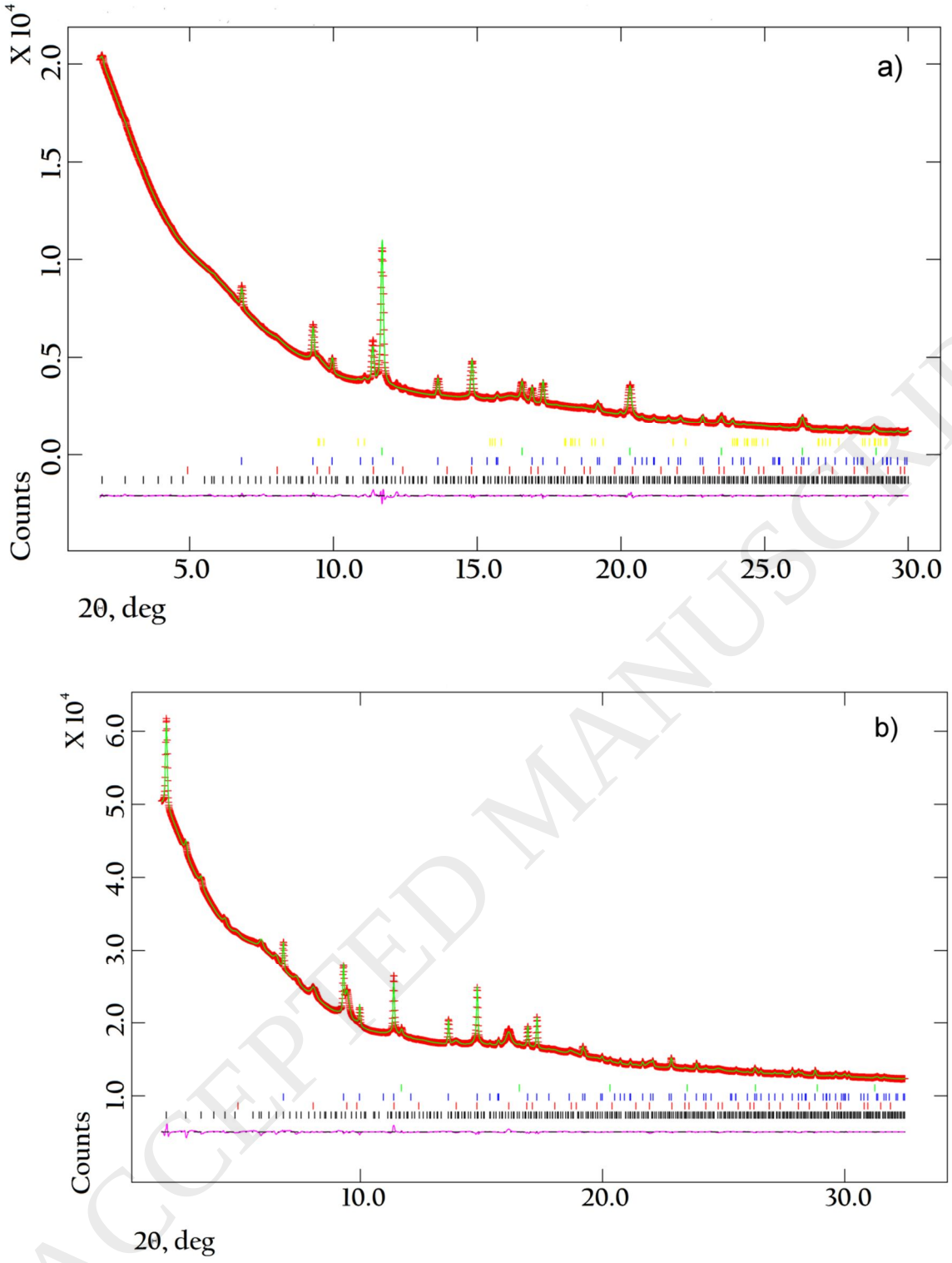

Figure 2

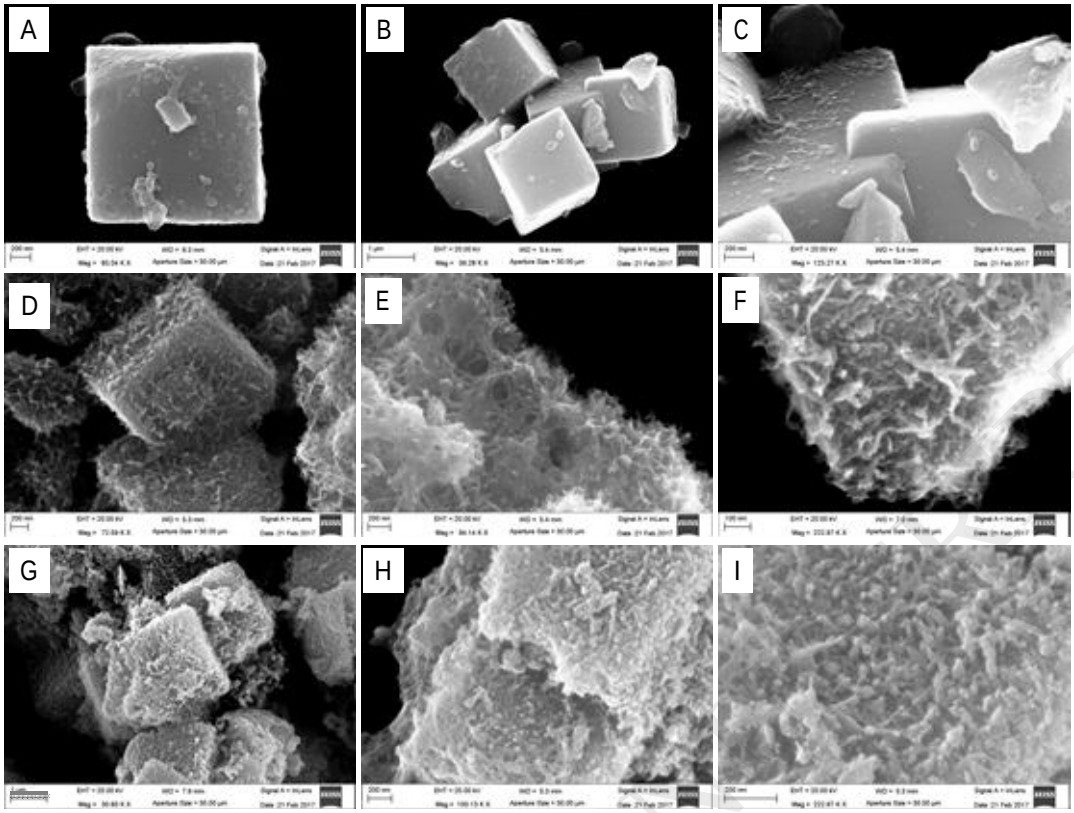

Figure 3

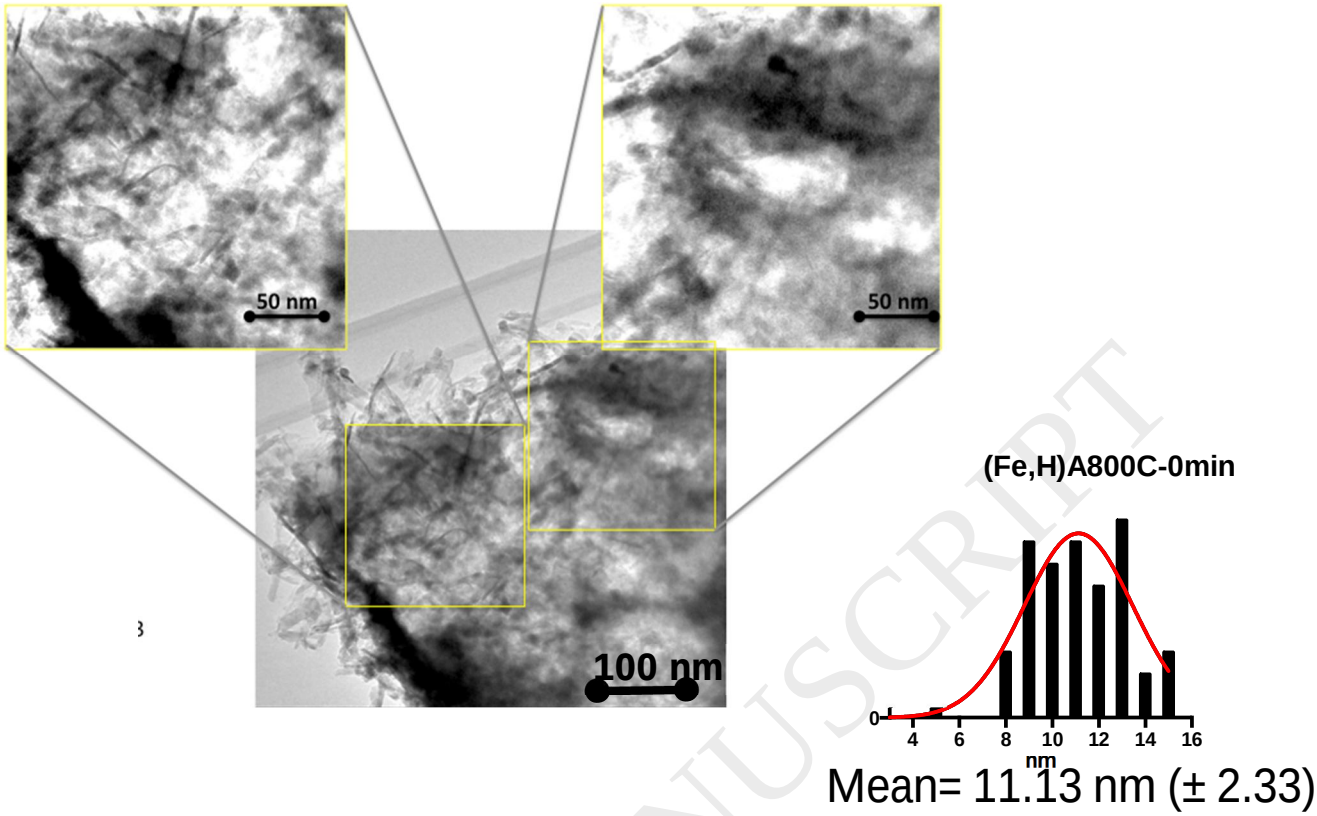

Figure 4A

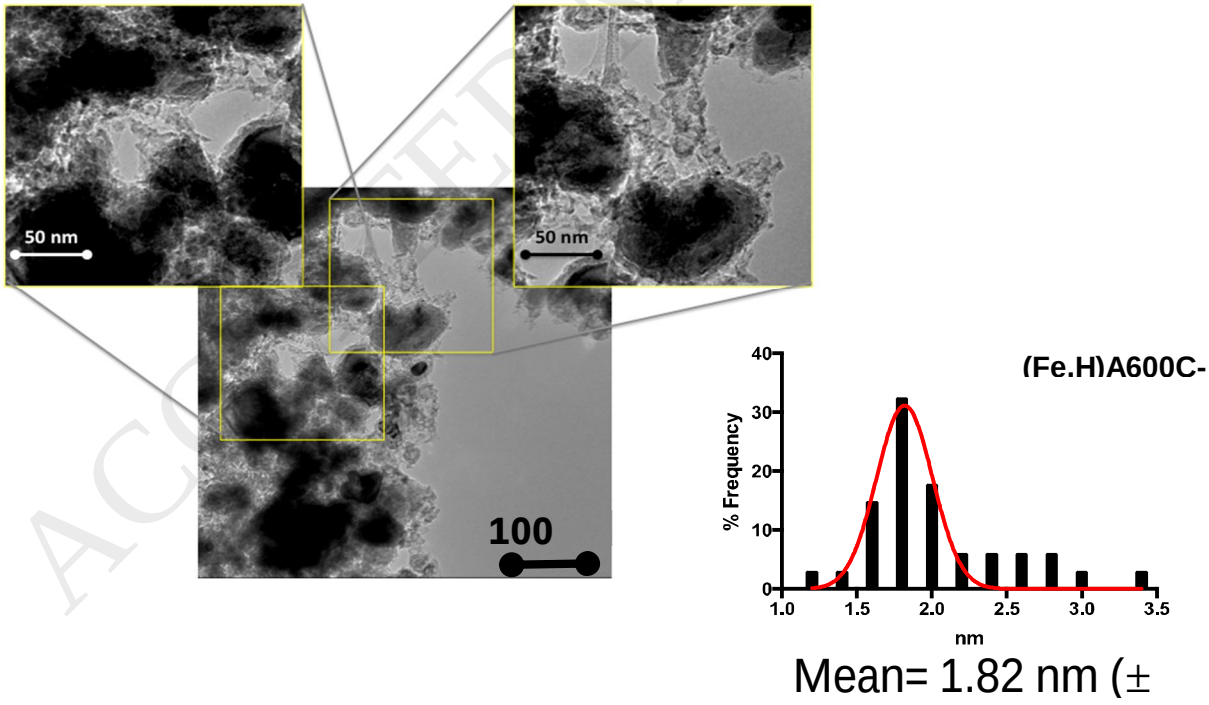

Figure 4B

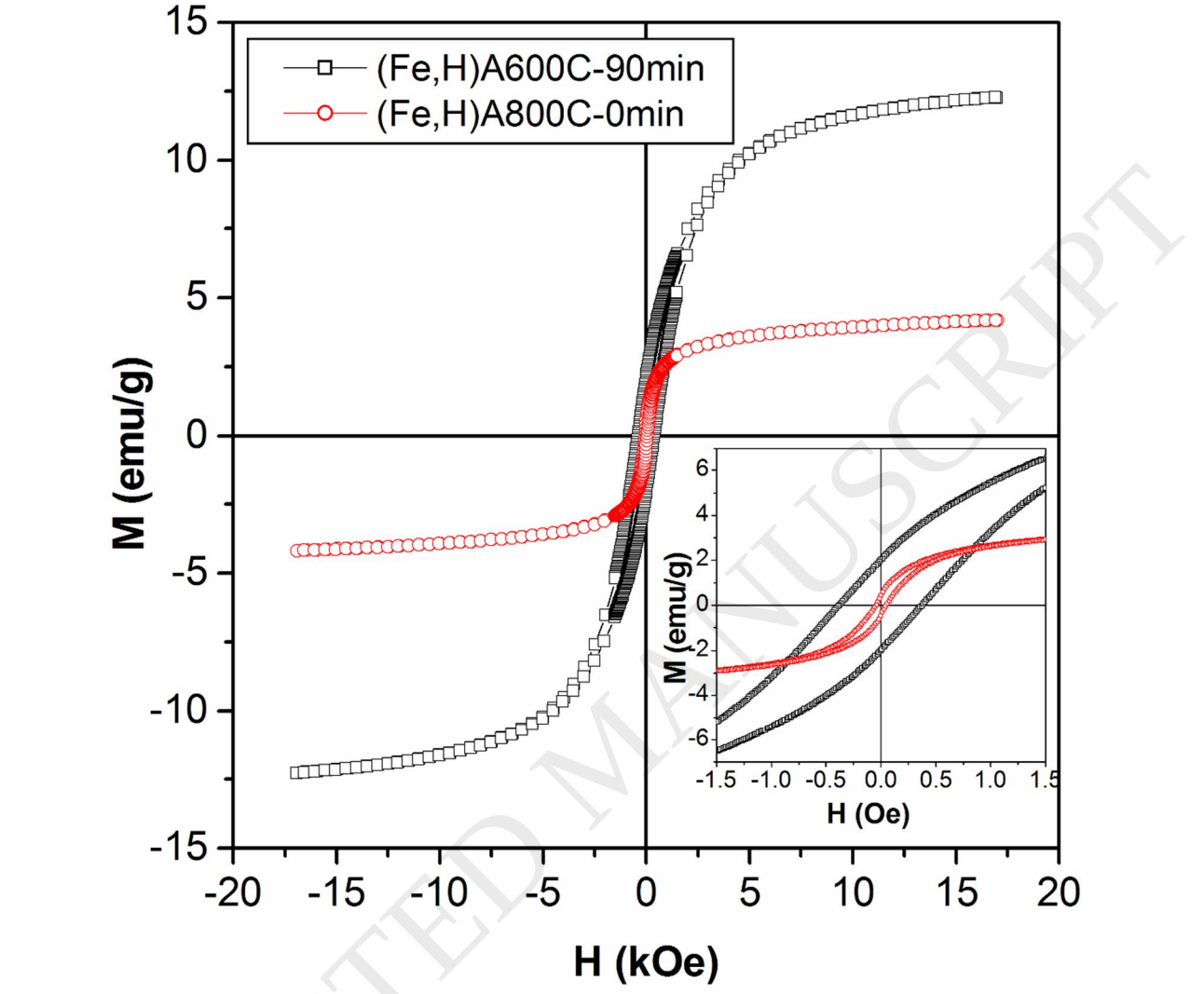

Figure 5

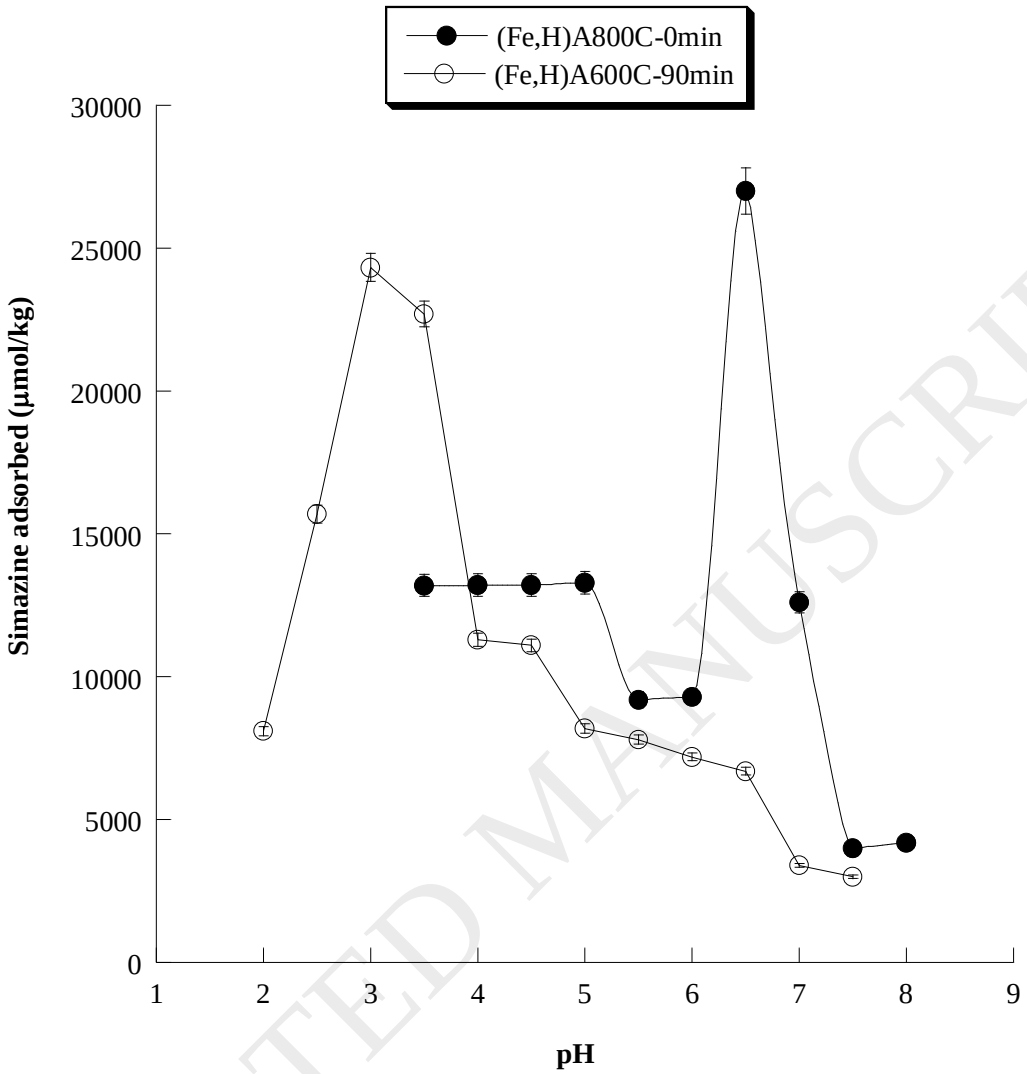

Figure 6

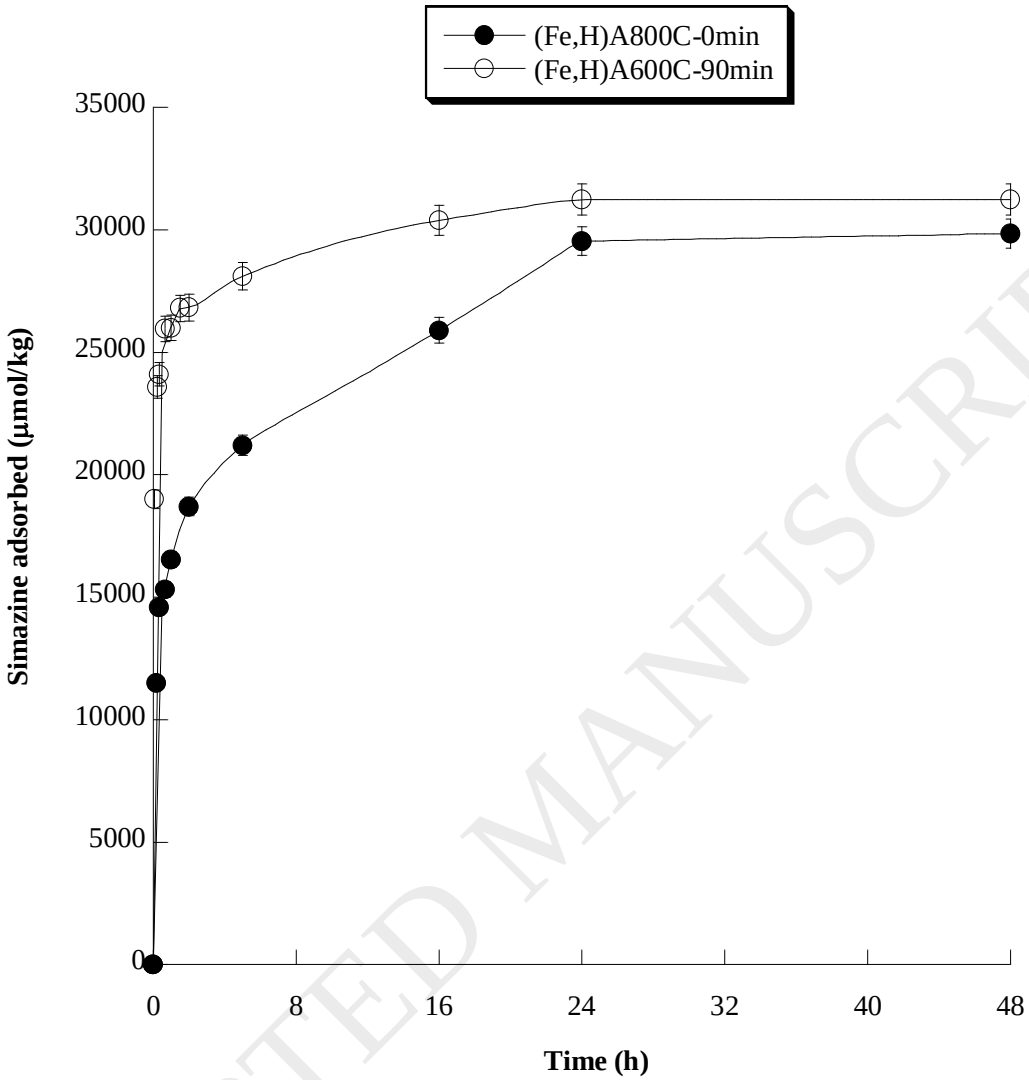

Figure 7

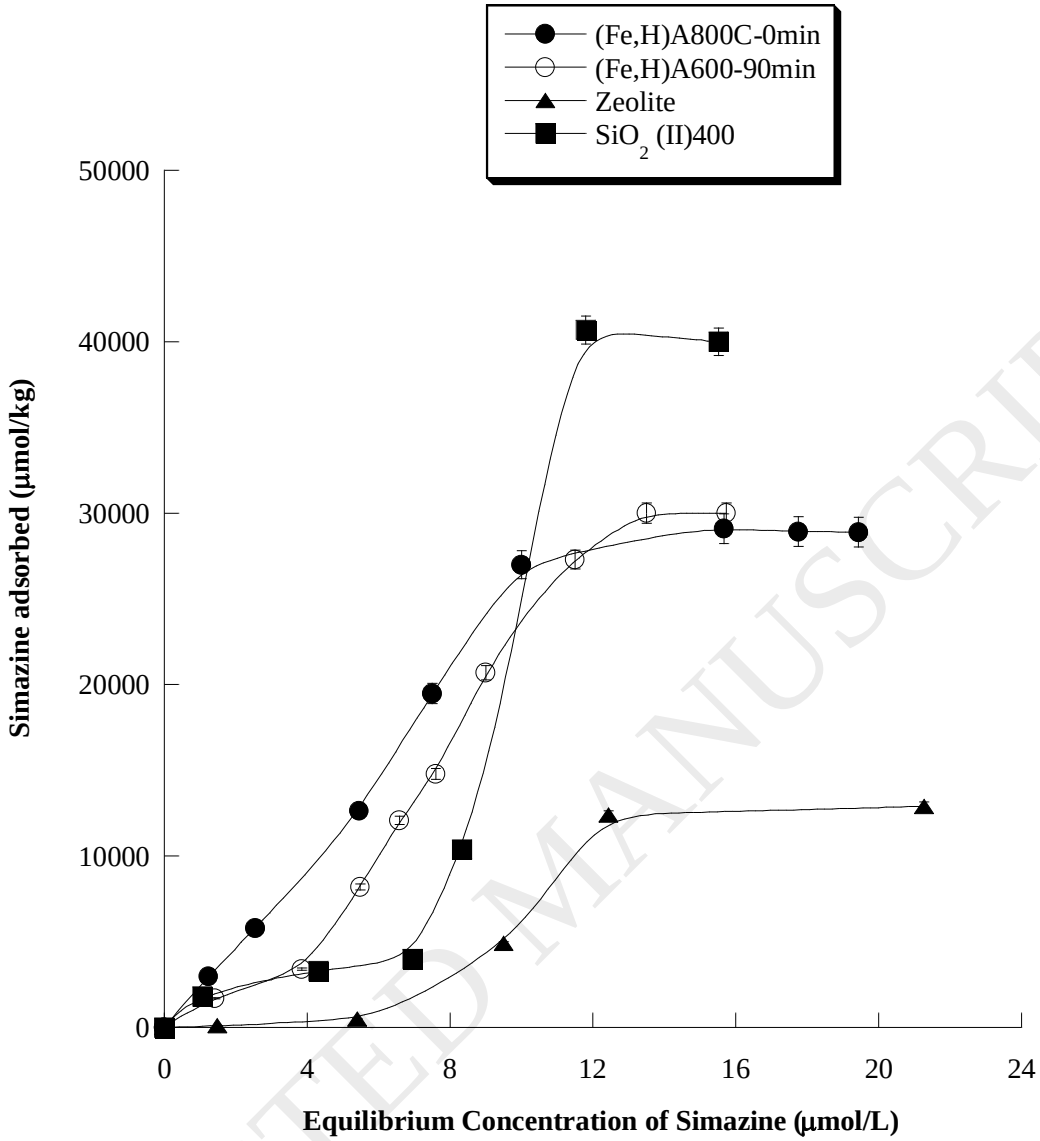

Figure 8

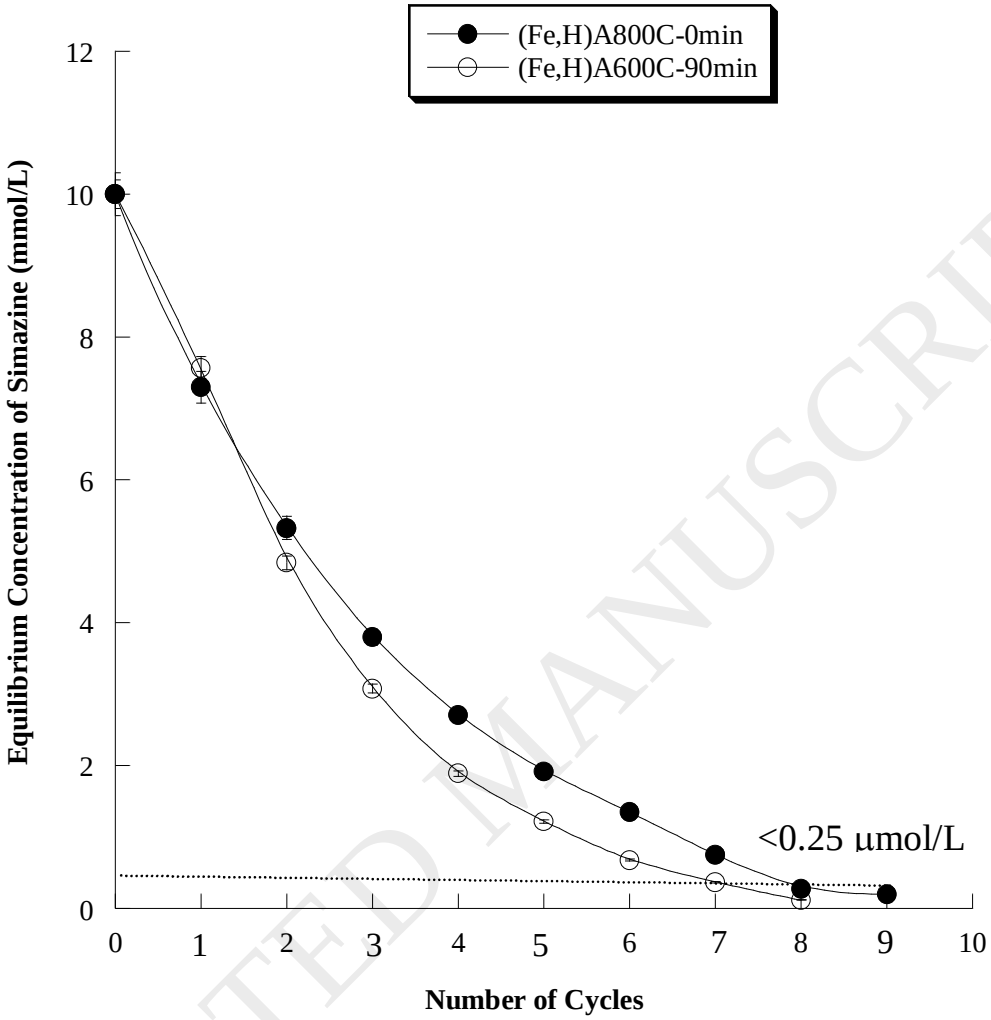

Figure 9

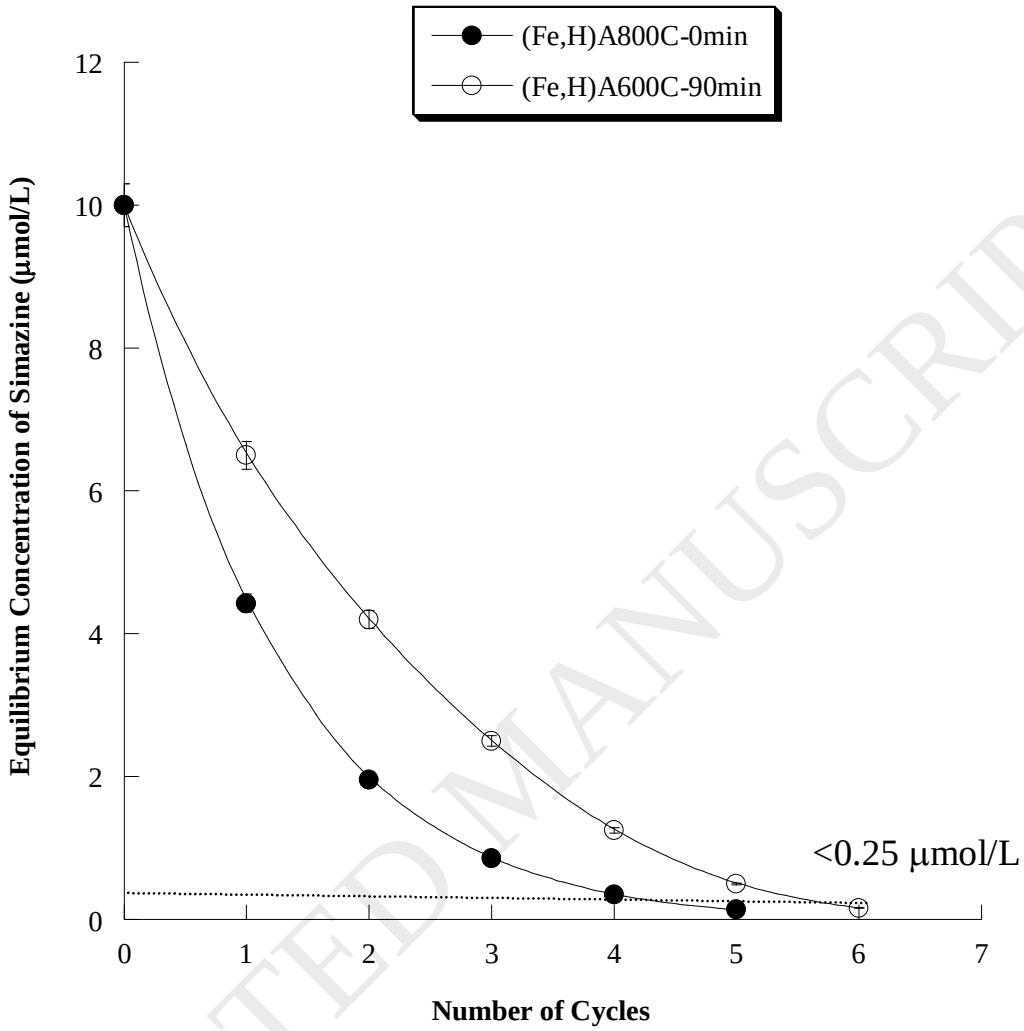

Figure 10